Aerosol and Air Quality
Research

ORIGINAL RESEARCH
https://doi.org/10.4209/aaqr.2020.07.0404

Source Apportionment of Urban Ammonia and its Contribution to Secondary Particle Formation in a Mid-size European City

Laura Ehrnsperger*, Otto Klemm

Climatology Research Group, Institute for Landscape Ecology, University of Münster, 48149 Münster, Germany

ABSTRACT

Ambient air pollution caused by fine particulate matter (PM) and trace gases is a pressing topic as it affects the vast majority of the world's population, with a particularly heavy influence in densely populated urban environments. Alongside nitrogen oxides (NO_x) and PM, ammonia (NH_3) is also a relevant air pollutant due to its role as a precursor of particulate ammonium. This is a study about the short-term temporal dynamics of urban NH_3 concentrations in Münster, northwest Germany, the role of road traffic and agriculture as NH_3 sources and about the importance of ammonia for secondary particle formation (SPF). The NH_3 mixing ratio was rather high (mean: 17 ppb) compared to other urban areas and showed distinct diurnal maxima around 10 a.m. and during the night at 9 p.m. The main source for ammonia in Münster was agriculture, but road traffic also contributed through local emissions from vehicle catalysts. NH_3 from surrounding agricultural areas accumulated in the nocturnal boundary layer and contributed to SPF in the city center. Modeled emissions of NH_3 as estimated by the Handbook for Emission Factors in combination with traffic counts were in the same magnitude for NH_3. The size-resolved chemical composition of inorganic ions in PM_{10} was dominated by NH_4^+ (8.66 $\mu g\ m^{-3}$), followed by NO_3^- (3.89 $\mu g\ m^{-3}$), SO_4^{2-} (1.58 $\mu g\ m^{-3}$) and Cl^- (1.33 $\mu g\ m^{-3}$). Particles in the accumulation range (diameter: 0.1–1 µm) showed the highest inorganic ion concentrations. The ammonium neutralization index J (111%) indicated an excess of NH_4^+ leading to mostly alkaline PM. High ammonia emissions from surrounding agricultural areas combined with large amounts of NO_x from road traffic play a crucial role for SPF in Münster.

Keywords: Ammonia sources, Road traffic, Agriculture, Urban air quality, Fine particulate matter

OPEN ACCESS

Received: July 15, 2020
Revised: November 20, 2020
Accepted: November 22, 2020

*** Corresponding Author:**
laura.ehrnsperger@wwu.de

Publisher:
Taiwan Association for Aerosol Research
ISSN: 1680-8584 print
ISSN: 2071-1409 online

1 INTRODUCTION

A vast majority of the world's population (91%) lives in locations that exceed the WHO air quality guidelines (WHO, 2016) with poor air quality responsible for one in every nine premature deaths in 2012 (WHO, 2016). Urban areas are especially prone to high levels of pollutants with an increasing frequency of air pollution episodes in many cities (WHO, 2016). This is due to the fact that the density of anthropogenic emission sources is higher in urban areas compared to rural regions. Air quality monitoring mainly focuses on particulate matter (PM), tropospheric ozone (O_3), and oxygenated N-, S-, and C-compounds including nitrogen oxides ($NO + NO_2 = NO_x$), sulfur dioxide (SO_2), and carbon monoxide (CO), while ammonia (NH_3), a reduced N-compound, is often neglected in urban air pollution monitoring and evaluation. Nevertheless, ammonia is the third most abundant N-species (Perrino *et al.*, 2002; Miller *et al.*, 2014) and negatively affects ecosystems via dry deposition, contributing to exceedances of nitrogen critical loads in oligotrophic environments (Aneja *et al.*, 2000; Sun *et al.*, 2017). Moreover, ammonia plays a special role in atmospheric air pollution as the main alkaline gas that neutralizes acidic compounds in the troposphere (Perrino *et al.*, 2002; Ferrara *et al.*, 2012), leading to the formation of secondary PM (e.g., $(NH_4)_2SO_4$, NH_4NO_3) (Perrino *et al.*, 2002), and enhancing the growth of existing particles (Baer *et al.*, 2012; Sun *et al.*, 2017; Wang *et al.*, 2020). SO_2 and NO_2 are the key gas-phase precursors of the acidic compounds (e.g., H_2SO_4, HNO_3) neutralized by ammonia and which are the primary components of secondary inorganic aerosols that dominate fine particle mass (e.g., Tsai *et al.*, 2014). It is therefore essential to understand secondary inorganic aerosol formation from precursor gases, including NH_3 (Tsai *et al.*, 2014). Because of their low molecular weights, NH_3 and NH_4^+ have a more significant impact on molar-based aerosol chemical and optical properties than the same mass of nitrate (NO_3^-), sulfate (SO_4^{2-}) or organic compounds (Sun *et al.*, 2017). NH_3-based secondary aerosols like NH_4NO_3 are furthermore essential for the long-range transport of acidic pollutants due to the longer lifetime of ammonium salts in the atmosphere (1–15 days) compared to pure gaseous NH_3 (few hours to few days) (Gordon, 1988; Aneja *et al.*, 2000; Dammers *et al.*, 2015). The main sources for NH_3 at continental to global scales are animal waste and fertilizers from high-intensity agriculture (Perrino *et al.*, 2002; Baer *et al.*, 2012; Sun *et al.*, 2017). In 32 member countries of the European Environment Agency (EEA), agriculture was responsible for over 90% of ammonia emissions into the atmosphere from 1990 to 2010 (EEA, 2010). Other sources are industries, biomass burning, humans, pets, wild animals, landfills and household products (Olivier *et al.*, 1998; Sutton *et al.*, 2000; Perrino *et al.*, 2002). The city of Münster lies within one of the hotspot areas of high ammonia concentrations due to its location in the so-called “swine belt”. This term describes the area of Northwest-Germany, Belgium and the Netherlands, where high-intensity animal husbandry of especially hog feeding is practiced. This leads to extremely high loads of local nitrogen deposition of 75 to 100 kg ha^{-1} y^{-1} in the Münsterland region, which lie above the mean N deposition for Germany (Frieling, 2014). The situation is similar for example to Taiwan (81% from agriculture, livestock and biogenic sources, 1% from traffic) (Tsai *et al.*, 2014), the North-China plain (88% from fertilizer application and livestock waste) (Zhang *et al.*, 2018) and the U.S. (86% from agricultural and natural sources, 8% from road traffic) (Livingston *et al.*, 2009). The contribution from vehicles was assumed to be negligible until 1995 in the U.S. (Eggleston, 1992; Sutton *et al.*, 1995; Perrino *et al.*, 2002), after which an increase in NH_3 traffic emissions occurred (Fraser and Cass, 1998; Moeckli *et al.*, 1996; Perrino *et al.*, 2002) in parallel to the increasing proportion of three-way catalytic converters (TWC) in gasoline vehicles from < 10% of the vehicle fleet in 1981 to > 75% in 1993 in the U.S. (Kean *et al.*, 2009). A similar pattern was observed for ammonia emissions from road transport in Italy after establishing TWCs (increase from < 1% in 1993 up to > 4% in 1999) (EEA, 2007). The NH_3 emission factor (EF) of vehicles in the U.S. increased from 1.3 ± 3.5 mg km^{-1} in 1981 (Pierson and Brachaczek, 1983) to 60 mg km^{-1} in 1993 (Fraser and Cass, 1998; Perrino *et al.*, 2002). Ammonia is emitted as a byproduct during the operation of TWCs (Wang *et al.*, 2019). A decreasing oxygen storage capacity of the catalyst caused by thermal aging in the TWC leads to overly reducing conditions in the catalyst and thereby increases the amount of produced NH_3 in the exhaust gas stream (Bielaczyc *et al.*, 2012). Besides TWCs, the selective catalytic reduction (SCR) systems of diesel vehicles have shown an increasing influence on ammonia emissions (Kean *et al.*, 2009). SCR catalysts use an aqueous solution called diesel exhaust fluid (32.5% urea, 67.5% deionized water) to convert NO_x in the exhaust stream to N_2 and water at temperatures between 150 and 350°C (formula (1)) (Boyce, 2012; Wang *et al.*, 2019).

$$4NH_3 + 2NO + 2NO_2 = 4N_2 + 6H_2O \tag{1}$$

To achieve this conversion the diesel exhaust fluid is permanently injected into the hot exhaust gas. The amount of diesel exhaust fluid is controlled by the vehicles’ software. Multiple studies showed that this process is working best, i.e., with a high conversion efficiency of 65% to 90%, under constant cruise speed and engine temperature (Boyce, 2012; Kim *et al.*, 2012). These conditions are often not met under real-world urban driving conditions leading to excess emissions of NO_x, PM and NH_3 from diesel vehicles (Fu *et al.*, 2013). The majority of diesel-fueled heavy-duty vehicles (HDVs) and light-duty vehicles (LDVs) in Europe was equipped with SCR catalysts from 2005 on (emission class Euro-IV) (Müller *et al.*, 2003), followed by passenger cars in 2015 (emission class Euro-6) to meet the NO_x limits of the European Union (Emitec GmbH, 2006). As a result of these developments, the traffic emissions of NH_3 are now 57% of the NO_x emissions in Germany (EEA, 2007). There have been attempts to reduce ammonia emissions in

Germany, but the actual decrease has been sparse (only 3% in the period from 1993 to 2009) (Ferm and Hellsten, 2012). In contrast to SO_2 or NO_x, which both decreased in the last decades due to effective regulations, there are no vehicle emission standards for NH_3 in Europe except the Euro-VI standard for diesel HDVs. Although ammoniated aerosols formed by secondary particle formation (SPF) are important for urban air quality, the emissions of their precursor gas ammonia are not well quantified or monitored (Sun *et al.*, 2017). Overall, the uncertainties of global NH_3 emissions are as large as 50% due to spatial and temporal variabilities and lack of *in-situ* measurement validation of emission inventories (Battye, 2003; Clarisse *et al.*, 2009; Moravek *et al.*, 2019). To account for the role of ammonia in the formation of fine PM, urban air pollution mitigation plans should also include reduction strategies for the primary precursor gas NH_3 which will help reduce SPF (Hanson *et al.*, 2002; Battye, 2003; McMurry *et al.*, 2005; Livingston *et al.*, 2009; Behera and Sharma, 2010; Benson *et al.*, 2011; Miller *et al.*, 2014). Attempts to monitor ammonia concentrations are often conducted at a low temporal resolution (Puchalski *et al.*, 2011). To fully characterize temporal NH_3 dynamics, measurements of ammonia with high temporal resolution are necessary (Battye, 2003; Nowak *et al.*, 2007; Pinder *et al.*, 2007; Miller *et al.*, 2014).

Münster is a typical medium-sized German city (~300,000 inhabitants) surrounded by intensive agricultural areas. This study aims 1) to identify ammonia emission sources at an urban site on different temporal scales from a few seconds to one day, 2) to evaluate the role of road traffic as an urban ammonia source using information from a real-world vehicle fleet combined with plume peak correlation of traffic-related trace gases with NH_3 and 3) to evaluate the role of ammonia in SPF by evaluating the chemical composition of size-resolved PM samples. Our analysis is based on data from a field campaign that we conducted in summer 2018 on an arterial road in the city center. The site is representative for the exposure of the urban German population to air pollution.

2 METHODS

2.1 Study Site

We conducted an experimental campaign by operating a measurement container next to a two-lane street in the city center of Münster, Germany (51.9635 N, 7.6313 E) from 30/08/2018 through 31/10/2018 (Fig. 1(a)). The road is an important East-West connection with a daily traffic volume of 33,700 vehicles and lies within a narrow street canyon with buildings of approximately nine to twelve meters height (height-to-width ratio ~0.56–0.75). The upper speed limit for road traffic was 30 km h^{-1}. A major local and regional bus station is located about 75 m to the NW, and a T-intersection with traffic lights is located about 60 m to the SE. The bus station is served by 19 public bus lines (Stadtwerke Münster, 2016b). The wind was channelled in the NW-SE direction by the street canyon (Fig. 1(b)). Mean wind speed was 1.0 m s^{-1} and the mean temperature was 20.7°C during the nine-week measurement period.

NO_2 is regularly monitored by the environmental protection agency of the federal state of North Rhine-Westphalia (LANUV NRW) by using passive samplers, which were about 18 m away from the measurement container (station code: VMSB). Annual average NO_2 concentration at the nearby air quality monitoring station (station code: VMSB) was 34.1 µg m^{-3} in 2018 (LANUV NRW, 2019). PM_{10} and NO_x are also monitored continuously by the LANUV NRW at the “Münster Weseler Straße” Station (station code: VMS2) 1.4 km beeline SW of the measurement container.

Münster is surrounded by intensively used agricultural areas, the nearest fields being located only 2.5 km beeline from the measurement container in the city center. Agriculture dominates the landscape outside the city (66% of the total area) (Lammers and Becker, 2014). The main crops are corn and several cereals (88% of total crops), which are both mostly used for animal husbandry (dairy farms, hog feeding, poultry farming) (Lammers and Becker, 2014).

2.2 Sampling

We collected meteorological and air pollution data on top of the measurement container. The sensors and sample inlets of wind speed and wind direction, air temperature, relative humidity (rH), CO_2, H_2O, NO_x, O_3, NH_3 and PM with diameters between 0.006 µm to 10 µm (PM_{10}) were located on top of the measurement container (horizontal distance to street: 0.3 m, height above ground: 4 m) (Table 1). The measurement frequency was 10 Hz, except for the ammonia instrument

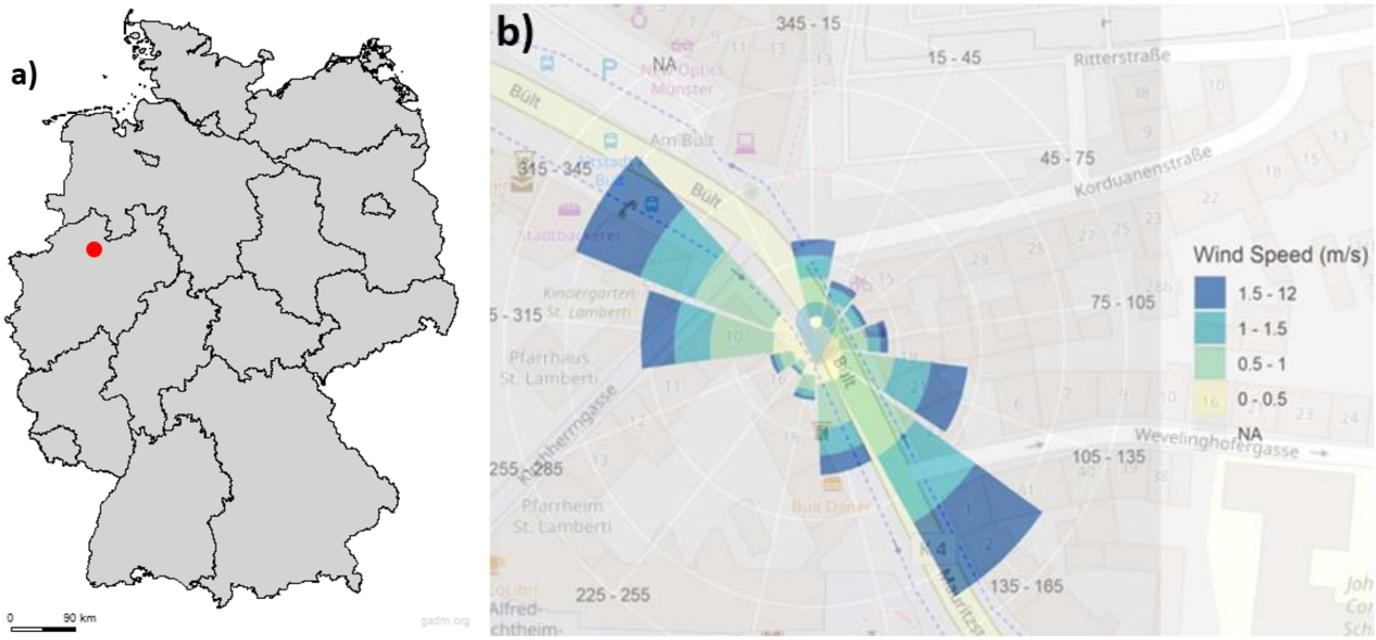

Fig. 1. (a) Map of Germany with borders of federal states. The city of Münster, North-Rhine Westphalia, is marked with a red point. (b) Detailed map of the measurement site located in a narrow street canyon. The location of the measurement container is indicated by the blue marker (source: Open Street Map). As a transparent overlay one can see the wind rose during the measurement campaign.

Table 1. Overview over all sensors used during the measurement campaign with the respective detection method and time resolution. The D50% separation diameters of the ELPI+ are 0.006, 0.017, 0.030, 0.060, 0.108, 0.17, 0.26, 0.40, 0.64, 1.0, 1.6, 2.5, 4.4, 6.8 and 10 µm, respectively.

Instrument	Parameter	Measurement technique	Time resolution	Height [m]
Gill RS3-50	Wind speed, wind direction, sonic temperature	3-D ultrasonic anemometer	10 Hz	4.40
LI-COR LI-7500A	CO_2, H_2O	Open-path NDIR gas analyzer	10 Hz	4.34
ECO PHYSICS CLD 899 Y	NO, NO_2	Chemiluminescence	10 Hz	4.04
ECO PHYSICS CLD 88	O_3	Chemiluminescence	10 Hz	4.03
Teledyne M501E	NH_3, NO, NO_2	Chemiluminescence	0.2 Hz	3.78
Dekati ELPI+	PMC, PNC for 14 size fractions	Electrical low-pressure impactor	10 Hz	3.96
Campbell Scientific HC2-S3	Air temperature, rH	Resistance thermometer	1 min	3.54

(0.2 Hz). CO_2 was quantified by measuring the absorptance of its molecules in the infrared spectrum over the open path of the LI-COR sensor head (sample column) (LI-COR Inc., 2009). The sensor head emits in the infrared spectrum and measures the remaining light intensity after the absorption by CO_2 molecules in the sample path at the detector unit. The more CO_2 is present in the sample path, the weaker is the detected infrared radiation signal at the detector unit. Ammonia was detected via the chemiluminescence technique, where NH_3 is oxidized into NO in a high-temperature catalytic converter at a temperature of 825°C and then the resulting NO is measured via by the chemiluminescent reaction with ozone at the detector unit (TAPI, 2012). To avoid a delayed or modified NH_3 signal, a stainless-steel tubing with a length of 1.3 m, permanently heated to 40°C, was employed. The Teledyne chemiluminescence detector was operated without a particulate filter to avoid adsorption and desorption from the filter depending on temperature and relative humidity. Due to the filter-less sampling setup NH_4^+ may contribute to the measured ammonia. The gas-to-particle-conversion ratio of ammonium and ammonia indicates that during the day, NH_3 is the major component, while during the night particulate NH_4^+ might also play a role. The high daytime temperatures during the measurement campaign probably lead to reliable measurements of NH_3 (Xu *et al.*, 2020). The effective time response of the system was 4 s. This time delay was removed in post-processing using cross-correlation with CO_2 as a traffic tracer. For NO_x and O_3, ambient air was sampled through thermally insulated PTFE tubing with 4.5 m and 3.9 m length, respectively. PM_{10} was collected with a Tygon tubing of 5 m length with an inner diameter of 10.5 mm at a flow rate of 10.5 L min^{-1}. PM samples (diameters: 0.05 µm–10 µm) were additionally collected with a five-stage-Berner impactor between 16/10/2018 and 23/10/2018 for 10 hours per day. PM was sampled on Tedlar foils for later inorganic ion analysis. As a measure for atmospheric static stability the stability parameter ζ was calculated using the meteorological data of the "Steinfurter Str." Station, which is operated by our research group, located 2.6 km beeline NW of the measurement container.

2.3 Traffic Detection

Automatic Number Plate Recognition (ANPR) cameras (model Long Range 25-1) (uniserve GmbH, Meschede, Germany) were installed at the measurement container to collect highly-resolved information on traffic density and vehicle characteristics. Video surveillance in public spaces was approved by the responsible data security officer in advance of this scientific study and in accordance with the EU data protection directive. Two cameras were orientated on one traffic lane each. During the nine weeks of measurements, a total of 841,568 vehicles were recorded. By license plate identification, information on vehicle type, engine type, European emission class, CO_2 emissions per km, etc. was obtained from the German Central Vehicle Register managed by the Federal Motor Transport Authority (Kraftfahrtbundesamt). For 6% of the recorded license plates, no vehicle characteristics were available either because they were from a foreign country or because the ANPR was faulty. Additionally, a microphone recorded the sound volume in the street canyon to test sound as a traffic indicator (Goulier *et al.*, 2020).

2.4 Data Processing and Time Series Analysis

A time series of 49 days of 0.2 Hz data was available for NH_3 with 86% of the data remaining for analysis after quality assessment and quality control (QA/QC). The 10 Hz data were available for a time series of 59 days, of which 99.3%, 96.7%, 96.6%, 77.4%, 73.4% and 97.4% passed the QA/QC procedure for the anemometer, CO_2, H_2O, NO_x, O_3 and PM_{10} data, respectively. All statistical computation and peak detection was performed with the open-source R version 3.5.1 (R Core Team, 2019) using the R-packages "openair" (Carslaw and Ropkins, 2012), "devtools" (Wickham *et al.*, 2020), "ggplot2" (Wickham, 2009), "gridExtra" (Baptiste, 2017), "stringi" (Gagolewski, 2020), "stringr" (Wickham, 2019), "data.table" (Dowle and Srinivasan, 2019), "padr" (Thoen, 2019), "egg" (Baptiste, 2019), "cowplot" (Wilke, 2019) and "OpenStreetMap" (Fellows and Stotz, 2019).

2.5 Peak Integration and Detection

Emissions from passing vehicles were detected as a peak of the respective air pollutants at the measurement site. The time lags caused by the tubing of enclosed-path sensors were quantified and eliminated by cross-correlation with the CO_2 concentration (time lag for NO_x, O_3 and PM were 3.6 s, 3.0 s and 4.0 s, respectively). Peak analysis of the data set was performed using the semi-empirical, automatic peak detection method of (Peitzmeier *et al.*, 2017). We assumed that each peak was caused by either an exhaust plume of a single vehicle or a combined exhaust plume. Peak integrals of all parameters were referenced to the simultaneously occurring peaks of CO_2. Peaks were defined as local maxima of the data record, for which 50 neighbouring points both prior and after the maximum were found. A total of 149,484 peaks were detected for CO_2, and the mean peak duration was 8.3 s (median: 6.3 s). The baseline for CO_2 was a moving median of 599 data points (1 min) with a moving standard deviation (SD) of 6000 data points (10 min) (Fig. 2). A moving average of 20 data points was calculated as the peakline (PL) following short-term variations of the CO_2 concentrations. The PL for NH_3 was calculated by a moving average of 12 data points (1 min) and the baseline with a moving median of 120 data points (10 min). When the baseline and the PL intersected, the segment of the time series was identified as a peak interval and the area of each pollutant was integrated for each peak interval. The integrated peak intervals were then used to compute the peak ratios of the respective component to CO_2. The concentrations of exhaust gases emitted by traffic will generally decrease with increasing

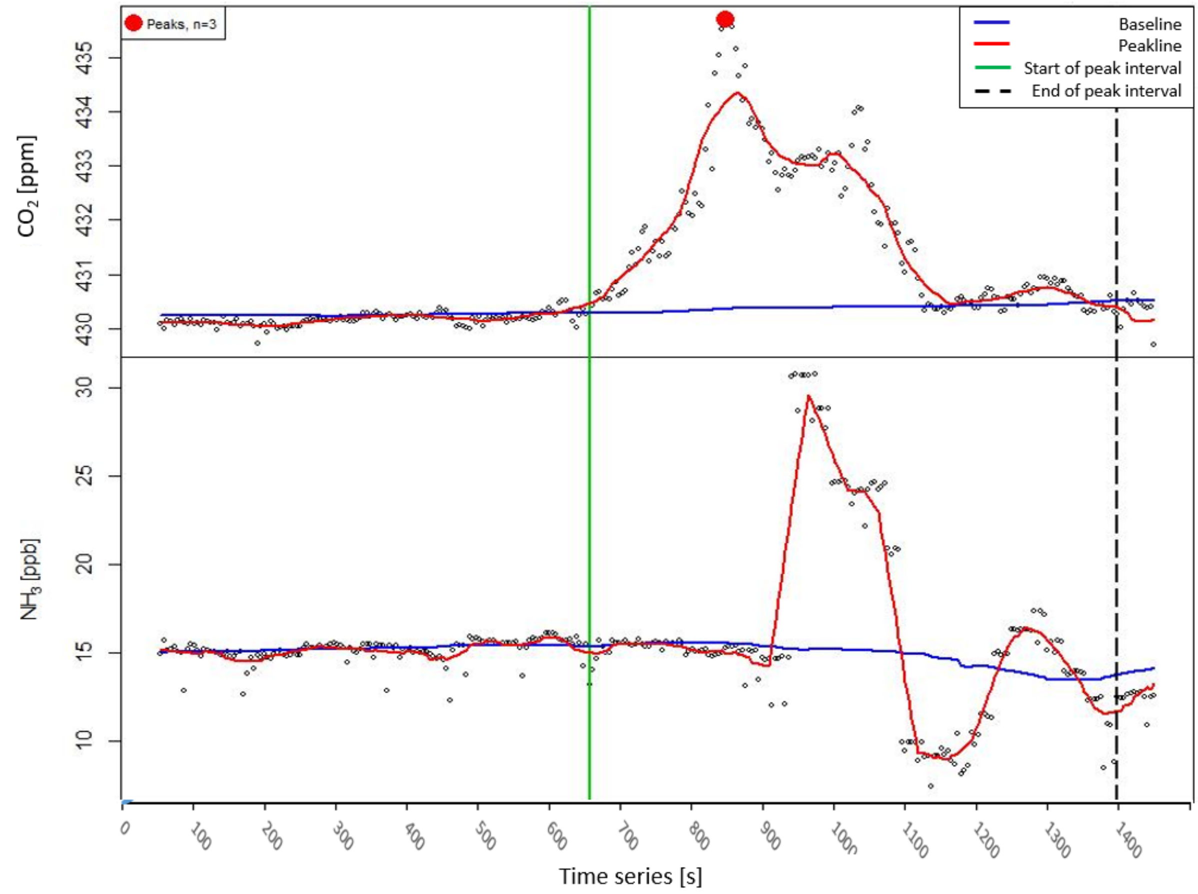

Fig. 2. Baselines (blue) and peaklines (red) of CO_2 (top panel) and NH_3 (bottom panel) for an example period of 1500 data points. The vertical green line represents the start of a peak and the vertical dashed black line indicates the end of a peak with the peak interval between the green and black line. The red point indicates an identified CO_2 peak, which was $\geq$ 3ppm.

distance from the source, but due to slow chemical reactions the ratio of the measured compounds will remain rather constant within a time period of several minutes to hours. Therefore, it is plausible to assume that the peak pollutant ratios measured at the measurement site are representative for the composition of exhaust plumes within the street canyon.

2.6 Handbook Emission Factors for Road Transport (HBEFA)

The HBEFA is a European database covering temperature-dependent emission factors for common vehicle types and traffic situations (Matzer *et al.*, 2019). Real-world emission measurements are used to model warm and cold start emissions depending on vehicle segment and traffic situation. The predicted emission factors of CO_2, CO_2 equivalents (CO_2e), NH_3, NO_x, NO_2, CO, CH_4, HC, NMHC, PM_{10} (for exhaust and non-exhaust), $PM_{2.5}$ (for exhaust and non-exhaust), particle number concentration for PM_{10} (PN_{10}), BC (for exhaust and non-exhaust) and SO_2 were computed for a comparable inner-city, stop-&-go traffic situation with a speed limit of 30 km h^{-1}, a typical German vehicle fleet composition, mean monthly temperatures for 2018 in Germany and an inclination of < 2% of the area. To compare the real-world ERs of road traffic with the theoretical emission ratios predicted by the HBEFA database, the air pollutant data and the traffic data were merged by timestamp. Therefore, each plume of air pollutants could be assigned to the respective vehicles that passed by the container during the same time period.

2.7 Chemical Analysis of Fine Particles

Fine particles collected with the five-stage Berner cascade impactor (stage 1: 0.05–0.14 µm, stage 2: 0.14–0.42 µm, stage 3: 0.42–1.2 µm, stage 4: 1.2–3.5 µm, stage 5: 3.5–10 µm) were analyzed for their concentration of sulfate, chloride, nitrate and ammonium. The sample foils were inserted into 50 ml vials and kept dry and frozen at –20°C until analysis. For the analysis, 10 mL of distilled water was added to each vial to extract the PM from the foils. The extracts were shaken for 1 h with 200 Mot min^{-1} and then ultrasonicated for another 1 h. Afterwards, each sample was filtered through a 0.22 µm pore size filter (Simplepure, NY + GF, 0.22 µm). NH_4^+ was analyzed with a continuous flow analyzer (Skalar, San++ Automated Wet Chemistry Analyzer) with a detection limit of 0.2 mg L^{-1}, and the concentrations of inorganic anions were measured using ion chromatography (Metrohm, 883 Basic IC plus) with a detection limit 0.5 mg L^{-1}.

3 RESULTS AND DISCUSSION

3.1 Peak Ratios of Air Pollutants in Exhaust Plumes from Road Traffic

The median peak ratios of NH_3/CO_2, NO_x/CO_2, PM_{10}/CO_2 and PN_{10}/CO_2 were calculated for synchronously detected peak intervals (Table 2). The overall median peak NH_3/CO_2 ratio was 6.11×10^{-5}, while the overall median peak NO_x/CO_2 ratio was 2.61×10^{-3} (Table 3). Thus, 43 times more NO_x was emitted per g CO_2 as compared to NH_3. The mass fraction of ammonia that is present in the vehicles' exhaust gas is apparently small compared to that of NO_x. For PM_{10}/CO_2 the median peak ratio (1.62×10^{-5}) was 26% of the median peak NH_3/CO_2 ratio. The PN_{10}/CO_2 ratio was 38829 p g^{-1}. The real-world (i.e., the *in-situ* measured variability during the measurement campaign) median peak NH_3/CO_2 ratio was 30% lower than the median peak NH_3/CO_2 emission ratio of HBEFA (8.70×10^{-5}) (Table 3). In addition, the variability of the real-world ammonia peak ratio was high compared to the HBEFA predictions for NH_3/CO_2 (Fig. 3). The interquartile range of the real-worldNH_3/CO_2 ratio was larger, but the median lower compared to the HBEFA median peak NH_3/CO_2 emission ratio. This indicates that the NH_3 emissions were distributed heterogeneously across the vehicle fleet in this study, where some vehicles caused very high short-term peaks of the NH_3 mixing ratio up to 216 ppb in the exhaust plumes, while other vehicles likely emitted much less or no ammonia at all. In a tunnel study in California, U.S., mainly light-duty vehicles (LDV) were responsible for traffic-related ammonia emissions, while heavy diesel trucks played only a minor role (Kean *et al.*, 2009). This was also likely the case at our study site, as the vehicle fleet during the measurement campaign consisted mainly of passenger cars and LDVs (91%) (Fig. 4). Busses and HDVs only make up for 6% and 3% of local road traffic, respectively (Fig. 4). They may be responsible for single NH_3 peaks, but overall their influence on traffic-related ammonia emissions are probably low. The second main factor influencing the amount of vehicle-emitted ammonia is the fuel type. Ammonia is mainly emitted by diesel vehicles due to selective catalytic reduction catalysts, which are used to clean the exhaust gas from NO_x using an urea solution (Eq. (1)) (Zhang and Wang, 2015). This reaction requires constant temperatures within

Table 2. Number of detected positive peak ratios of NH_3/CO_2, NO_x/CO_2, PM_{10}/CO_2 and PN_{10}/CO_2 for the measurement campaign, respectively.

Peak ratio [g g^{-1}]	Nr. peak intervals [-]
NH_3/CO_2	1784
NO_x/CO_2	88428
PM_{10}/CO_2	40456
PN_{10}/CO_2	36898

Table 3. Median peak emission ratios of the detected peak intervals of NH_3/CO_2 [g g^{-1}], NO_x/CO_2 [g g^{-1}], PM_{10}/CO_2 [g g^{-1}] and PN_{10}/CO_2 [p g^{-1}] for the measurement campaign and the HBEFA database, respectively.

Parameter	HBEFA	Real-world
NH_3/CO_2	8.70×10^{-5}	6.11×10^{-5}
NO_x/CO_2	4.06×10^{-4}	2.61×10^{-3}
PM_{10}/CO_2	8.04×10^{-6}	1.62×10^{-5}
PN_{10}/CO_2	5252701539	38829

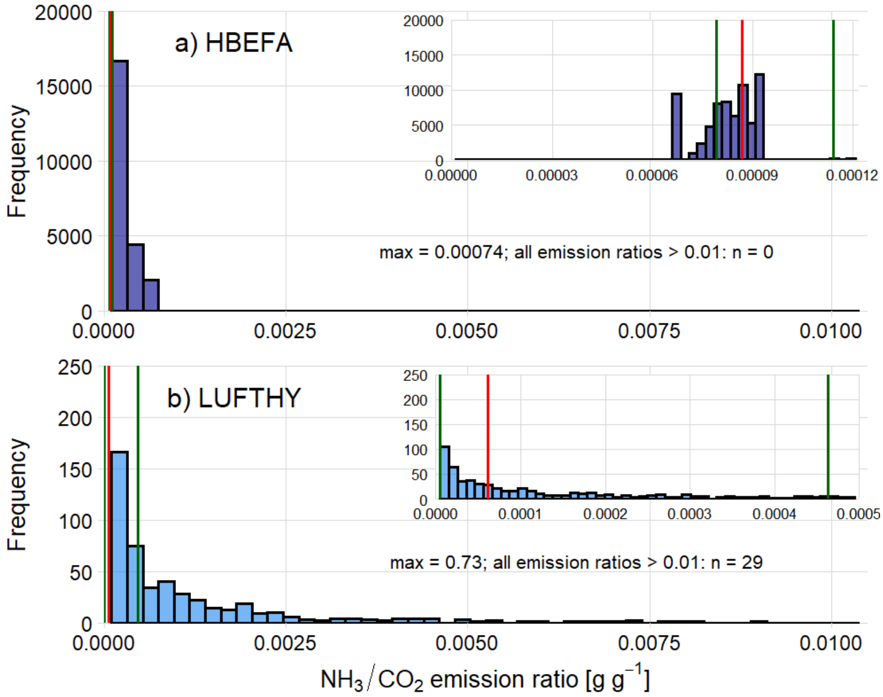

Fig. 3. Median peak NH_3/CO_2 ratios for the theoretical predictions of the HBEFA (a) and for the measurement campaign (b) based on the local vehicle fleet. Each inlet subplot shows the interquartile ranges of the respective NH_3/CO_2 ratios. The vertical dark green lines represent the 1st and 3rd interquartile range limits and the vertical red line indicates the median value of the real-world NH_3/CO_2 ratio and the HBEFA NH_3/CO_2 emission ratio.

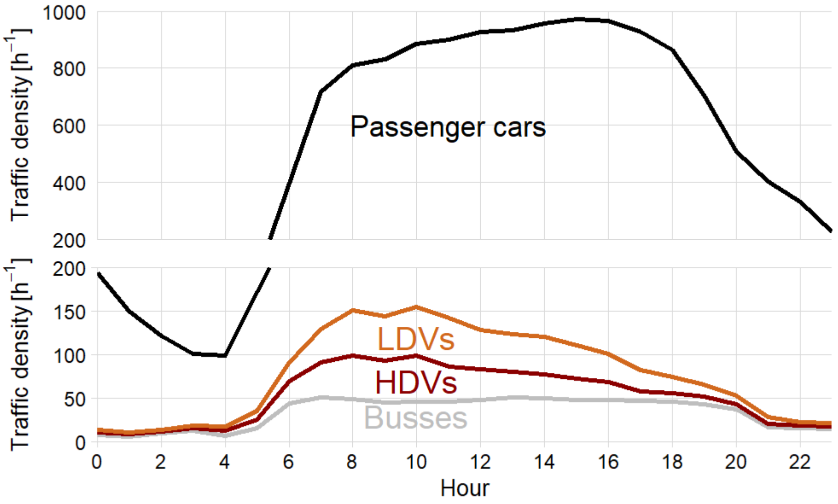

Fig. 4. Mean diurnal cycle of the vehicle types during the campaign. The curves of busses (beneath the grey line), HDVs (beneath the dark red line), LDVs (beneath the orange line) and passenger cars (beneath the black line) are additive summing up to the overall traffic density (black line). Please note that the y-axis is broken with a different y-axis scaling for the upper and bottom panel to show the patterns of HDVs, LDVs and busses despite their small share on the overall traffic density.

the catalyst and an adjusted amount of injected urea solution. Both requirements are often not met during urban driving conditions with frequently changing cruising speeds and cold-started engines. Additionally, the tanks containing the diesel exhaust fluid are often designed too small to provide an adequate amount on long-term operation. Moreover, vehicle manufacturers manipulated the vehicles' software to reduce the use of diesel exhaust fluid in order to decrease vehicle weight and avoid the need of frequent refills of the urea solution. So, the vehicles with so-called 'defeat devices' only met the air pollution restrictions on the test bench, but not under real-world driving conditions. The shutdown of SCR catalysts leads to less emissions of NH_3, but increased emissions of nitrogen oxides from the respective vehicles. This incident became known as the Dieselgate scandal in 2015 and was one of the greatest intentional deceptions of consumers so far (Bovens, 2016). In Europe, 8.5 Mio. vehicles had manipulated SCR catalysts of the manufacturer "Volkswagen" (VW), of which 2.5 Mio. were registered in Germany (BMVI, 2016). In our study, vehicles with SCR catalysts make up 19% of the vehicle fleet. TWC systems of gasoline vehicles also emit NH_3 if the catalyst is thermally aged. Hybrid vehicles are promoted as an environmental-friendly alternative to conventional fuels, but depending on the fuel used, they can also contribute significantly to traffic-related ammonia emissions. A hybrid vehicle with a TWC was shown to emit 93% more ammonia when it was operated with gasoline compared to Compressed Natural Gas (CNG) as an alternative power source, while another vehicle emitted 2% more NH_3 when fueled with liquefied petroleum gas (LPG) (Bielaczyc *et al.*, 2012). Besides vehicle type, also the driving patterns can significantly influence NH_3 emissions. Several dynamometer laboratory studies have revealed that ammonia emissions were highest during acceleration events of modern vehicles (Huai *et al.*, 2003, 2005). Bielaczyc *et al.* (2012) also found a correlation between engine power and ammonia emissions. Therefore, it is likely that high short-term NH_3 emissions occurred during the typical urban stop and go traffic.

The peak detection method by Peitzmeier *et al.* (2017) proved to be valuable to estimate real-world peak ratios of NH_3/CO_2, NO_x/CO_2, PM_{10}/CO_2 and PN_{10}/CO_2. Nevertheless, the method has some limitations. The respective second air pollutant (NH_3, NO_x, PM_{10}, PN_{10}) has to peak in the same peak interval as CO_2 or it will not be detected and thus no peak ratio will be calculated. A given exhaust plume may reach the open-path CO_2 analyzer, but not the inlet for the other analyzers (NH_3, NO_x, PM), although the distance between them was small (56 cm, 30 cm, 38 cm). Also, the vehicles' exhaust plumes may mix on their way to the sensor inlets leading to indistinctive peak signals representing a number of vehicles rather than a single one. In addition, a certain fraction of plumes may not have been detected at all as they did not pass the instruments' inlets due to meteorological conditions (adverse wind direction, etc.). In consequence, there is a considerable uncertainty in the peak assignment to vehicles. On the other hand, it is the sheer number of analyzed peaks (149,484 CO_2 peaks) populating the emission dataset that yielded statistically robust and overall reliable data.

3.2 Source Apportionment of NH_3 in the Urban Atmosphere

The NH_3 mixing ratios in an urban street canyon in Münster, NW Germany, during the measurement campaign were rather large (mean: 17 ppb, median: 15 ppb) compared to those found in other studies, for instance with averages ranging from 1.1 ppb in Houston, U.S. (Nowak *et al.*, 2010) to 12 ppb in Seoul, Korea (Phan *et al.*, 2013). The NH_3 mixing ratio at road level during our study (median: 15 ppb) was furthermore three-times higher than the ammonia mixing ratio measured in Münster at a rooftop upwind of the city center in 2005 (median: 5.2 ppb) (Vogt *et al.*, 2005). This indicates that emissions from motorized road traffic contribute significantly to NH_3 at our urban study site, in addition to those of the intensively cultivated agricultural areas that surround the city (Vog *et al.*, 2005). Note that chemical and physical processes such as nucleation, volatilization and wet and dry deposition lead to a complex temporal pattern of NH_3 responding to emissions, wind direction, wind speed, temperature, rH as well as boundary layer (BL) dynamics. The mean diurnal cycle of the ammonia mixing ratio showed a distinct diel course with a maximum at 1000 and a daily amplitude of 9 ppb (Fig. 5). It is striking that this late morning maximum was not synchronous with the increase of traffic nor with the peaks of the other trace gases and particles. CO_2 and NO_x, but also PM_{10} and PN_{10} begin increasing early in the morning at 0600 and reach their maxima at 0800 (Fig. 5). After the steep increase during morning rush hour, CO_2, NO_x, PM_{10} and PN_{10} decrease after 0800, although the traffic density kept increasing slightly until 1700. After a stable atmospheric BL during the night, the new daily mixed layer developed after 0800. At the same time, the NO_x, CO_2, PM_{10} and PN10 mixing ratios and concentrations begin to decrease as less polluted air is entrained into the mixed layer from above. Meanwhile, NH_3 also increases and reaches its peak mixing ratio at 1000, when the BL is least stable with a

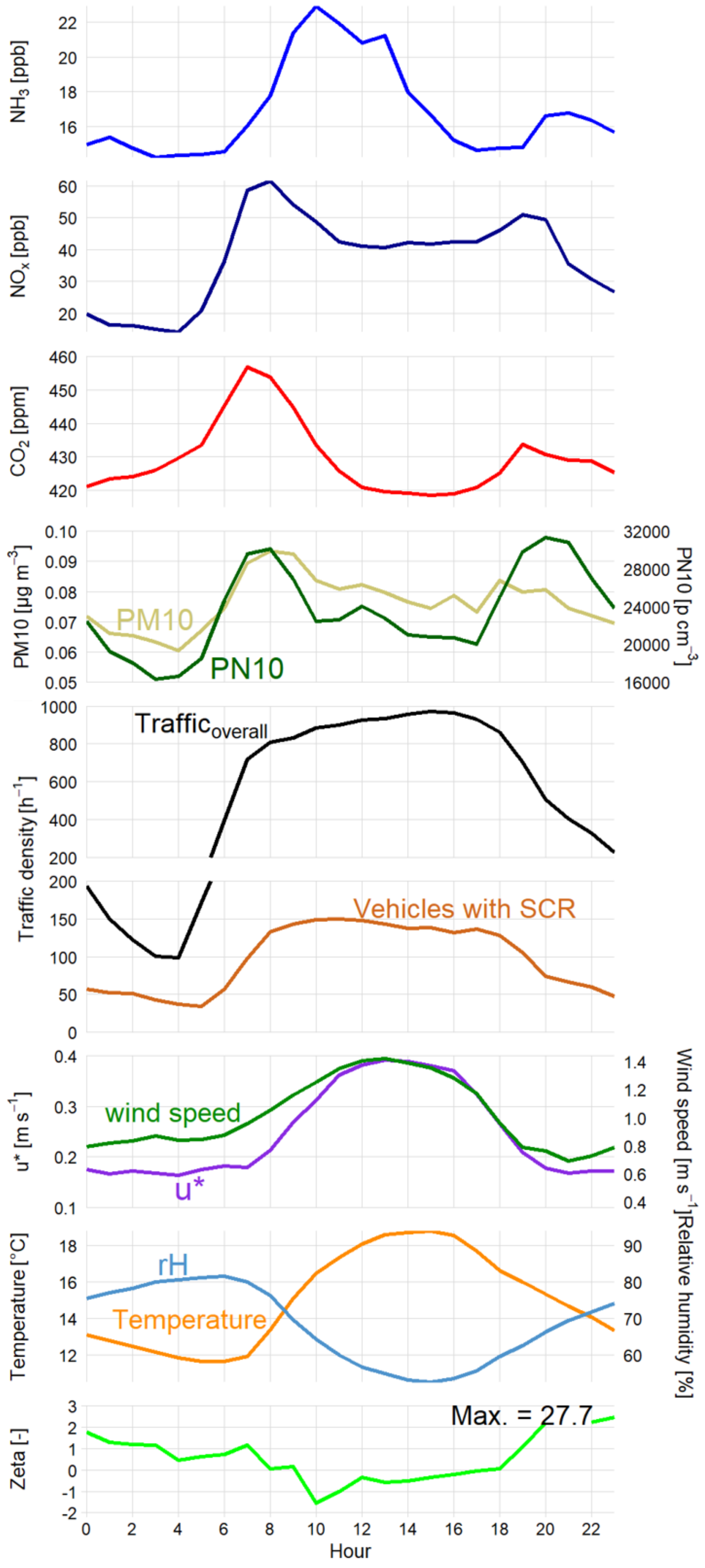

Fig. 5. Mean diurnal cycle of NH_3, CO_2, NO_x, PM_{10}, PN_{10}, traffic density, wind speed, friction velocity u* and stability parameter zeta ζ. Please note that the y-axis for the traffic density plot is broken with a different y-axis scaling for the upper and bottom panel to show the patterns of overall road traffic and vehicles with SCR-catalysts despite their small share on the overall traffic density.

stability parameter ζ of –1.57. A plausible explanation could be that ammonia had not been homogeneously mixed within the nocturnal residual layer, but was enriched in its upper parts. As soon as the atmospheric conditions transitioned from stable to neutral and unstable (0800–1000), the accumulated NH_3 caused the midday peak after getting entrained into the mixed layer. This process is a good explanation for the observed diurnal pattern of NH_3 and indicated that ammonia must have its origin outside the city, in the agricultural surroundings of Münster. There was also an increase of SCR-equipped vehicles in the late morning hours (Fig. 4), but the percentage of these vehicle on the overall traffic volume is so low that their contribution to overall ammonia emissions is likely to be only of minor importance.

It is surprising, though, that the high NH_3 mixing ratio did not persist after 1000. The rather rapid decrease of ammonia mixing ratio in the afternoon may have been caused by removal or dilution of NH_3 in the mixed layer. The concentrations of all traffic-related air pollutants and of NH_3 decreased during the afternoon until 1800 as the mixing layer further developed, although the traffic intensity stayed high throughout this period (Fig. 5). After the stabilization of the BL at 1800, the respective concentrations picked up again. NH_3, NO_x, CO_2, PM_{10} and PN_{10} mixing ratios and concentrations showed second maxima during the early night hours. NO_x and CO_2 peaked soon after the stabilization of the boundary layer at 1900, while NH_3, PM_{10} and PN_{10} had their nocturnal maxima around 2000. This pattern was likely caused by the less pronounced mixing within the nocturnal boundary layer during stable atmospheric conditions combined with a still high traffic density. Gong *et al.* (2011) also observed a similar diurnal NH_3 cycle during August 2010 to September 2010 with a morning peak at 1100, a decrease during midday and a nighttime increase. This diurnal cycle has been typical for urban ammonia concentrations in many cities (Olszyna *et al.*, 2005; Sudheer and Rengarajan, 2015). A nighttime peak of PM was also observed in an urban, industrial area of southern Taiwan, where the nocturnal maximum even exceeded the daytime peak (Tsai *et al.*, 2014).

Note that air temperature and rH apparently had no influence on the temporal dynamics of NH_3 in Münster, which contradicts most previous studies (Baek *et al.*, 2004; Behera and Sharma, 2010; Shen *et al.*, 2011). This missing correlation between air temperature and rH and ammonia concentrations was observed for Münster before (Vogt *et al.*, 2005). If vaporization of particulate NH_4^+ was important, an increase of gaseous NH_3 should have occurred during increasing temperature and decreasing rH until 1600, but that was not the case. Nevertheless, the high overall mean NH_3 mixing ratio may have been influenced by the increased volatilization of ammonia due to high air temperatures during the measurement campaign (mean: 20.7°C). A seasonal pattern with higher NH_3 concentrations during summer was for example observed in central Taiwan (Lin *et al.*, 2006) and mainland China (Shen *et al.*, 2011). The mean wind speed during the nine-week campaign was relatively low (1.0 m s^{-1}) (Fig. 1(b)), so, the transport of air out of the street canyon was not very pronounced. Therefore, emission sources were apparently more important than meteorological conditions.

The pollutant ratios during daytime and nighttime peaks can give insight into the sources of the pollutants (Table 4). If the pollutant ratios of the two daily peaks differ, it is likely that the daytime and nighttime sources are also not identical. The midday NH_3/NO_x peak ratio was 3.2 times higher (0.121 g g^{-1}) compared to the nighttime ratio (0.038 g g^{-1}). Also, the NH_3/CO_2 peak ratio was 1.5 times higher during daytime. This higher daytime ratio of NH_3/NO_x and NH_3/CO_2 supports our assumption that agriculture was the main ammonia source during the day.

Thus, during stable atmospheric conditions at night, both NH_3 and NO_x were emitted mainly from catalysts of both gasoline and diesel vehicles. Together with the high amount of ammonia present due to agricultural activities the excess NO_x degrades the urban air quality in Münster and has potentially negative impacts on human health.

Table 4. Median peak emission ratios of the detected peak intervals of NH_3/CO_2, NO_x/CO_2, NH_3/NO_x for the measurement campaign during daytime and nighttime, respectively.

Emission ratio [g g^{-1}]	Daytime	Nighttime
NH_3/CO_2	1.03×10^{-4}	6.90×10^{-5}
NO_x/CO_2	8.52×10^{-4}	1.82×10^{-3}
NH_3/NO_x	1.21×10^{-1}	3.80×10^{-2}

3.3 Contribution of Ammonia to PM Formation

Ammonia is an important gas-phase precursor for PM due to its ability to form particulate ammonium salts (Perrino *et al.*, 2002; Kirkby *et al.*, 2011). Given the high ammonia mixing ratio during the measurement campaign, NH_3 likely contributed significantly to the formation of secondary PM in the urban air. The analysis of inorganic ions showed that the ammonium ion did indeed play an important role in the inorganic PM composition across all particle sizes with diameters from 0.05 µm to 10 µm (five size ranges) (Fig. 6). NH_4^+ was even the major component in the accumulation mode of PM ranging from 0.14 µm to 0.71 µm in diameter. The reactions of gaseous NH_3 with acidic gases (left-hand sides of reactions (2) and (3)) to form particulate NH_4^+ (right-hand sides of reactions (2) and (3)) played apparently an essential role for PM formation in Münster (reactions (2) and (3)).

$$NH_3 + H_2SO_4 \leftrightarrow NH_4HSO_4 \tag{2}$$

$$NH_3 + HNO_3 \leftrightarrow NH_4NO_3 \tag{3}$$

This finding is in good correspondence with our former result that the main sources for NH_3 at the site are emissions by surrounding agricultural activities. The high amounts of ammonium in the accumulation mode of PM point to medium-range transported particles from rural areas outside the city. Ammonium was also found to be the major inorganic ion in accumulation-mode PM collected in Münster at a site upwind of the city (Vogt *et al.*, 2005). A study in the U.S. observed a synchronous increase in ammonia and ammonium around mid-day indicating that NH_3 contributes to aerosol particle mass (Gong *et al.*, 2013). Ammonia was also identified as important for SPF in India (Behera and Sharma, 2010), Japan (Sakurai and Fujita, 2002; Aikawa *et al.*, 2005), Korea (Phan *et al.*, 2013), mainland China (Hu *et al.*, 2008; Shen *et al.*, 2011) and Taiwan (Tsai *et al.*, 2014). The second most abundant inorganic ion components in PM were nitrate and sulfate, followed by chloride (Fig. 6). A study in Taiwan found a similar contribution of water-soluble ionic species to PM with NH_4^+ especially dominant in the size range from 0.1 µm to 1 µm (78%) (Tsai *et al.*, 2014). Nitrate and sulfate both stem from the combustion of fossil fuels, while chloride originates from sea salt aerosol. As the temperatures during the measurement period were relatively high and domestic heating thus very low, it is likely that road traffic was a major source for particulate NO_3^- and SO_4^{2-} during the day in Münster. The locally emitted exhaust compounds then react with the gaseous ammonia, which originated mostly from agricultural areas outside the city. Studies from central and southern Taiwan concluded that nitrate concentrations might be even higher during the night, when NO_3^- is thermally more stable (Lin *et al.*, 2006; Tsai *et al.*, 2014). Former measurements of inorganic ion concentrations in Münster (Vogt *et al.*, 2005) support the presumption that the concentrations of secondary inorganic PM were likely higher during

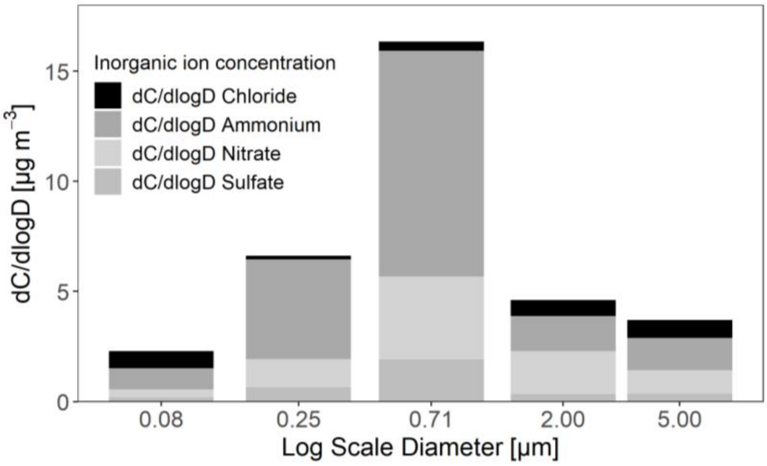

Fig. 6. Chemical composition of PM collected with the Berner Impactor. The stacked bar plots show the concentrations of the inorganic anions nitrate, sulfate and chloride and the cation ammonium.

nighttime also in our case. Additionally, it is probable that nitrate and sulfate were transported into the city in the form of ammonium salts. This process would explain the coincidental dominance of ammonium, nitrate and sulfate in the accumulation range particle fraction (Fig. 6).

The mean molar ratio (MMR) of NH_4^+/SO_4^{2-} gives insight on the abundance of ammonia with respect to its potential to neutralize H_2SO_4 (Behera and Sharma, 2010; Seinfeld and Pandis, 2016). Behera and Sharma (2010) found that the formation of $(NH_4)_2SO_4$ is favoured (S-conversion ratio = F_S: 58%) over the formation of NH_4NO_3 (N-conversion ratio = F_n: 39%). The PM in Münster showed a MMR of 2.7 for NH_4^+/SO_4^{2-}. Mean molar ratios > 2 indicate that high amounts of excess ammonia are available for chemical reactions other than the formation of $(NH_4)_2SO_4$. It is therefore likely that, in addition to the formation of ammonium sulfate and ammonium bisulfate, also high amounts of NH_4NO_3 are formed in Münster. Our results are similar with those from an urban site in India (MMR of $NH_4^+/SO_4^{2-} = 2.8$) (Behera and Sharma, 2010) and one in southern Taiwan (MMR of $NH_4^+/SO_4^{2-} = 3.2$) (Tsai *et al.*, 2014), which both observed ammonium-rich aerosol. To further assess the capability of ammonia to neutralize not only H_2SO_4, but also HNO_3, the ammonium neutralization index J for the collected PM was calculated.

$$J = \frac{\left[NH_4^+\right]}{2 \times \left[SO_4^-\right] + \left[NO_3^-\right]} \times 100\% \tag{4}$$

when $J < 100\%$ a NH_4^+ deficit is present, while at $J = 100\%$ the particles are neutral, and for $J > 100\%$ there is an excess of ammonium with the consequence that PM tends to be alkaline. Unfortunately, the complete charge balance could not be calculated due to missing measurements of the cations besides NH_4^+ (K^+, Ca^{2+}, Na^+), but ammonium is assumed to be dominant at the site. The J index was 113% for the PM samples collected during our campaign, which is comparable to a study in India reporting a J index of 111% (Behera and Sharma, 2010). Thus, there was a distinct excess of NH_4^+ present at the measurement site in the city center of Münster. As ammonia is so abundant, the reduction of NH_3 emissions would have to be massive to achieve a detectable effect on air quality. Therefore, it might be more promising on the short-term to further reduce other traffic-related compounds like NO_x and SO_2. If these limiting compounds are not present for the reaction with ammonia, no ammonium salts can be produced and the SPF is suppressed. Nevertheless, a long-term reduction of ammonia will be beneficial not only for urban air quality, but also to remedy other environmental issues (eutrophication of natural ecosystems, pollution of groundwater and streams).

4 CONCLUSIONS

Overall, the typical dynamic stop and go driving pattern at the urban site led to highly variable peak emissions of NH_3 in Münster. The real-world emissions of NH_3 are similar to the theoretical emissions predicted by the HBEFA, but under real-world conditions the variance across the vehicle fleet was greater. TWC systems of gasoline vehicles and SCR catalysts of diesel engines are responsible for these local emissions of NH_3. All in all, road traffic was only a minor source for ammonia in Münster. The mean diurnal mixing ratios revealed that the main source of NH_3 was emissions from agricultural activities. Ammonia was transported from rural areas into the city and accumulated in the residual layer above the city during the night. In the late morning hours, NH_3 was mixed into the urban BL as soon as the dynamic atmospheric stability became unstable. Despite its origin, ammonia has important implications for the air quality in Münster. Ammonium was an important component of PM in the size fractions from 0.05 µm to 10 µm together with nitrate and sulfate, indicating that ammonium salts were a major component of inorganic PM at the urban site. The interplay of combustion emissions from traffic (NO_x, SO_2) and NH_3 from agriculture has important implications for particle formation and particle dynamics. To effectively enhance urban air quality, besides sulfur and nitrogen oxides, also ammonia emissions have to be reduced. This claim is not unique for Münster, but also valid for many other regions as e.g., China (Shen *et al.*, 2011) or the U.S. (Pinder *et al.*, 2007). Backes *et al.* (2016) estimated that a 50% reduction of NH_3 emissions would result in a reduction of $PM_{2.5}$ concentrations up to 25% in winter. In the case of Münster, the atmosphere is so rich in ammonia that it would be more effective to further reduce its reaction partners NO_x and SO_2 in order to enhance air quality on a short-term perspective. This suggests the further promotion of SCR catalyst systems to reduce traffic-related NO_x because that reduces the formation of PM more than the additional emissions of NH_3 associated with it will increase it. On the long-term, it is nevertheless advisable to reduce agricultural ammonia emissions. Paulot and Jacob (2014) estimated that the reduction of NH_3 from livestock operations would lead to greater health benefits than the decrease of National Ambient Air Quality Standards for $PM_{2.5}$ from 15 μm^3 to 12 μm^3 in the U.S. All in all, policymakers and municipalities should include emissions from agriculture into urban air pollution mitigation plans to successfully enhance air quality in cities.

The semi-empirical peak detection method successfully estimated real-world peak ratios of NH_3/CO_2. The method has some limitations due to possible time delays of the respective peaks of the different air pollutants and transport pathways of the exhaust plumes, but the large number of analysed plumes led to robust conclusions with respect to the vehicle fleet that passed the measurement site during the experimental period.

ACKNOWLEDGMENTS

We like to thank the German Research Foundation (DFG) for founding this project (Project-ID: KL 623/21-1). We are furthermore grateful to Laura Goulier and Bastian Paas, who helped with field work during the measurement campaign. We also acknowledge the cooperation with the municipalities of the city of Münster. We thank Stephen M. Griffith for language editing of the manuscript and two anonymous reviewers of an earlier version of the manuscript, who helped to improve it significantly.

DISCLAIMER

The authors have no conflict of interest concerning the scope of this study.

REFERENCES

Aikawa, M., Hiraki, T., Tamaki, M. (2005). Characteristics in concentration of chemical species in ambient air based on three-year monitoring by filter pack method. Water Air Soil Pollut. 161, 335–352. https://doi.org/10.1007/s11270-005-4774-9

Aneja, V.P., Chauhan, J.P., Walker, J.T. (2000). Characterization of atmospheric ammonia emissions from swine waste storage and treatment lagoons. J. Geophys. Res. 105, 11535–11545. https://doi.org/10.1029/2000JD900066

Backes, A.M., Aulinger, A., Bieser, J., Matthias, V., Quante, M. (2016). Ammonia emissions in Europe, part II: How ammonia emission abatement strategies affect secondary aerosols. Atmos. Environ. 126, 153–161. https://doi.org/10.1016/j.atmosenv.2015.11.039

Baek, B.H., Aneja, V.P., Tong, Q. (2004). Chemical coupling between ammonia, acid gases, and fine particles. Environ. Pollut. 129, 89–98. https://doi.org/10.1016/j.envpol.2003.09.022

Baer, D., Gupta, M., Leen, J.B., Berman, E. (2012). Environmental and Atmospheric Monitoring Using Off-Axis Integrated Cavity Output Spectroscopy (OA-ICOS). American Laboratory. http://www.americanlaboratory.com/913-Technical-Articles/125787-Environmental-and-Atmospheric-Monitoring-Using-Off-Axis-Integrated-Cavity-Output-Spectroscopy-OA-ICOS/ (accessed 27 November 2017).

Baptiste, A. (2017). gridExtra: Miscellaneous Functions for "Grid" Graphics. R package version 2.3. https://CRAN.R-project.org/package=gridExtra

Baptiste, A. (2019). egg: Extensions for 'ggplot2': Custom Geom, Custom Themes, Plot Alignment, Labelled Panels, Symmetric Scales, and Fixed Panel Size. R package version 0.4.5. https://CRAN.R-project.org/package=egg

Battye, W. (2003). Evaluation and improvement of ammonia emissions inventories. Atmos. Environ. 37, 3873–83. https://doi.org/10.1016/S1352-2310(03)00343-1

Behera, S.N., Sharma, M. (2010). Investigating the potential role of ammonia in ion chemistry of fine particulate matter formation for an urban environment. Sci. Total Environ. 408, 3569–3575. https://doi.org/10.1016/j.scitotenv.2010.04.017

Benson, D.R., Yu, J.H., Markovich, A., Lee, S.H. (2011). Ternary homogeneous nucleation of H_2SO_4, NH_3, and H_2O under conditions relevant to the lower troposphere. Atmos. Chem. Phys. 11, 4755–4766. https://doi.org/10.5194/acp-11-4755-2011

Bielaczyc, P., Szczotka, A., Swiatek, A., Woodburn, J. (2012). A Comparison of ammonia emission factors from light-duty vehicles operating on gasoline, liquefied petroleum gas (LPG) and compressed natural gas (CNG). SAE Int. J. Fuels Lubr. 5, 751–759. https://doi.org/10.4271/2012-01-1095

Boyce, M.P. (2012). 10 - Combustors, in: Boyce, M.P. (Ed.), Gas Turbine Engineering Handbook (Fourth Edition), Butterworth-Heinemann, Oxford, pp. 427–490. https://doi.org/10.1016/B978-0-12-383842-1.00010-X

Bundesministerium für Verkehr und digitale Infrastruktur (BMVI) (2016). Berichte der Untersuchungskommission „Volkswagen“. https://www.bmvi.de/blaetterkatalog/catalogs/235222/pdf/save/bk_1.pdf

Carslaw, D.C., Ropkins, K. (2012). openair — An R package for air quality data analysis. Environ. Modell. Software 27–28, 52–61. https://doi.org/10.1016/j.envsoft.2011.09.008

Clarisse, L., Clerbaux, C., Dentener, F., Hurtmans, D., Coheur, P.F. (2009). Global ammonia distribution derived from infrared satellite observations. Nat. Geosci. 2, 479–483. https://doi.org/10.1038/ngeo551

Dammers, E., Vigouroux, C., Palm, M., Mahieu, E., Warneke, T., Smale, D., Langerock, B., Franco, B., Van Damme, M., Schaap, M., Notholt, J., Erisman, J.W. (2015). Retrieval of ammonia from ground-based FTIR solar spectra. Atmos. Chem. Phys. 15, 12789–12803. https://doi.org/10.5194/acp-15-12789-2015

Dowle, M., Srinivasan, A., Gorecki, J., Chirico, M., Stetsenko, P., Short, T., Lianoglou, S., Antonyan, E., Bonsch, M., Parsonage, H., Ritchie, S., Ren, K., Tan, X., Saporta, R., Seiskari, O., Dong, X., Lang, M., Iwasaki, W., Wenchel, S., Broman, K., … Schwen, B. (2019). data.table: Extension of “data.frame.” R package version 1.12.8. https://CRAN.R-project.org/package=data.table

Eggleston, H.S. (1992). An improved U.K. ammonia emission inventory. Laxenburg, Austria: IIASA. pp. 95–107.

Emitec GmbH (2006). Perspectives on Mobile SCR Technology. With the assistance of E. Jacob.

European Environment Agency (EEA) (2007). Air pollution in Europe 1990 - 2004: EEA Report. No 2/2007. http://www.env-edu.gr/Documents/Air%20pollution%20in%20Europe%201990%E2%80%932004.pdf

European Environment Agency (EEA) (2010). Ammonia (NH_3) emissions. https://www.eea.europa.eu/data-and-maps/indicators/eea-32-ammonia-nh3-emissions-1

Fellows, I., Stotz, J.P. (2019). OpenStreetMap: Access to Open Street Map Raster Images. R package version 0.3.4. Using the JMapViewer library by Jan Peter Stotz. https://CRAN.R-project.org/package=OpenStreetMap

Ferm, M., Hellsten, S. (2012). Trends in atmospheric ammonia and particulate ammonium concentrations in Sweden and its causes. Atmos. Environ. 61, 30–39. https://doi.org/10.1016/j.atmosenv.2012.07.010

Ferrara, R.M., Loubet, B., Di Tommasi, P., Bertolini, T., Magliulo, V., Cellier, P., Eugster, W., Rana, G. (2012). Eddy covariance measurement of ammonia fluxes: Comparison of high frequency correction methodologies. Agric. For. Meteorol. 158–159, 30–42. https://doi.org/10.1016/j.agrformet.2012.02.001

Fraser, M.P., Cass, G.R. (1998). Detection of excess ammonia emissions from in-use vehicles and the implications for fine particle control. Environ. Sci. Technol. 32, 1053–1057. https://doi.org/10.1021/es970382h

Frieling, D. (2014). Wirkung von Stickstoff-Einträgen auf die Umwelt: Situation in NRW. Fachgespräch Stickstoffbilanzen, 2014.

Fu, M., Ge, Y., Wang, X., Tan, J., Yu, L., Liang, B. (2013). NO_x emissions from Euro IV busses with SCR systems associated with urban, suburban and freeway driving patterns. Sci. Total Environ. 452–453, 222–226. https://doi.org/10.1016/j.scitotenv.2013.02.076

Gagolewski, M. (2020). R package stringi: Character string processing facilities. http://www.gagolewski.com/software/stringi/

Gong, L., Lewicki, R., Griffin, R.J., Flynn, J.H., Lefer, B.L., Tittel, F.K. (2011). Atmospheric ammonia measurements in Houston, TX using an external-cavity quantum cascade laser-based sensor. Atmos. Chem. Phys. 11, 9721–9733. https://doi.org/10.5194/acp-11-9721-2011

Gong, L., Lewicki, R., Griffin, R.J., Tittel, F.K., Lonsdale, C.R., Stevens, R.G., Pierce, J.R., Malloy, Q.G.J., Travis, S.A., Bobmanuel, L.M., Lefer, B.L., Flynn, J.H. (2013). Role of atmospheric ammonia in particulate matter formation in Houston during summertime. Atmos. Environ. 77, 893–900. https://doi.org/10.1016/j.atmosenv.2013.04.079

Gordon, G.E. (1988). Chemistry of the natural atmosphere. Peter Warneck. Academic Press, San Diego, CA, 1988. xiv, 757 pp., illus. $85. International Geophysics Series, vol. 41. Science 242, 121–122. https://doi.org/10.1126/science.242.4875.121-a

Goulier, L., Paas, B., Ehrnsperger, L., Klemm, O. (2020). Modelling of urban air pollutant concentrations with artificial neural networks using novel input variables. Int. J. Environ. Res. Public Health 17, 2025. https://doi.org/10.3390/ijerph17062025

Hanson, D.R., Eisele, F.L., Ball, S.M., McMurry, P.M. (2002). Sizing small sulfuric acid particles with an ultrafine particle condensation nucleus counter. Aerosol Sci. Technol. 36, 554–559. https://doi.org/10.1080/02786820252883793

Hu, M., Wu, Z., Slanina, J., Lin, P., Liu, S., Zeng, L. (2008). Acidic gases, ammonia and water-soluble ions in $PM_{2.5}$ at a coastal site in the Pearl River Delta, China. Atmos. Environ. 42, 6310–6320. https://doi.org/10.1016/j.atmosenv.2008.02.015

Huai, T., Durbin, T.D., Miller, J.W., Pisano, J.T., Sauer, C.G., Rhee, S.H., Norbeck, J.M. (2003). Investigation of NH_3 emissions from new technology vehicles as a function of vehicle operating conditions. Environ. Sci. Technol. 37, 4841–4847. https://doi.org/10.1021/es030403+

Huai, T., Durbin, T.D., Younglove, T., Scora, G., Barth, M., Norbeck, J.M. (2005). Vehicle specific power approach to estimating on-road NH_3 emissions from light-duty vehicles. Environ. Sci. Technol. 39, 9595–9600. https://doi.org/10.1021/es050120c

Kean, A.J., Littlejohn, D., Ban-Weiss, G.A., Harley, R.A., Kirchstetter, T.W., Lunden, M.M. (2009). Trends in on-road vehicle emissions of ammonia. Atmos. Environ. 43, 1565–1570. https://doi.org/10.1016/j.atmosenv.2008.09.085

Kim, Y.J., Kwon, H.J., Heo, I., Nam, I.-S., Cho, B.K., Choung, J.W., Cha, M.-S., Yeo, G.K. (2012). Mn–Fe/ZSM5 as a low-temperature SCR catalyst to remove NO_x from diesel engine exhaust. Appl. Catal., B 126, 9–21. https://doi.org/10.1016/j.apcatb.2012.06.010

Kirkby, J., Curtius, J., Almeida, J., Dunne, E., Duplissy, J., Ehrhart, S., Franchin, A., Gagné, S., Ickes, L., Kürten, A., Kupc, A., Metzger, A., Riccobono, F., Rondo, L., Schobesberger, S., Tsagkogeorgas, G., Wimmer, D., Amorim, A., Bianchi, F., Breitenlechner, M., … Kulmala, M. (2011). Role of sulphuric acid, ammonia and galactic cosmic rays in atmospheric aerosol nucleation. Nature 476, 429–433. https://doi.org/10.1038/nature10343

Lammers, Marianne, and Thorsten Becker (2014). Landwirtschaft im Münsterland: Daten - Fakten - Analysen. 2. Auflage

LI-COR Inc. (2009). LI-7500A Open Path CO_2/H_2O Analyzer Instruction Manual. Publication NO. 984-10563.

Lin, Y., Cheng, M., Ting, W., Yeh, C. (2006). Characteristics of gaseous HNO_2, HNO_3, NH_3 and particulate ammonium nitrate in an urban city of Central Taiwan. Atmos. Environ. 40, 4725–33. https://doi.org/10.1016/j.atmosenv.2006.04.037

Livingston, C., Rieger, P., Winer, A. (2009). Ammonia emissions from a representative in-use fleet of light and medium-duty vehicles in the California South Coast Air Basin. Atmos. Environ. 43, 3326–3333. https://doi.org/10.1016/j.atmosenv.2009.04.009

Matzer, C., Weller, C., Dippold, M., Lipp, S., Röck, M., Rexeis, M., Hausberger, S. (2019). Update of Emission Factors for HBEFA Version 4.1: Final report. I-05/19/CM EM-I-16/26/679.

McMurry, P.H., Fink, M., Sakurai, H., Stolzenburg, M.R., Mauldin, R.L., Smith, J., Eisele, F., Moore, K., Sjostedt, S., Tanner, D., Huey, L.G., Nowak, J.B., Edgerton, E., Voisin, D. (2005). A criterion for new particle formation in the sulfur-rich Atlanta atmosphere. J. Geophys. Res. 110, D22S02. https://doi.org/10.1029/2005JD005901

Miller, D.J., Sun, K., Tao, L., Khan, M.A., Zondlo, M.A. (2014). Open-path, quantum cascade-laser-based sensor for high-resolution atmospheric ammonia measurements. Atmos. Meas. Tech. 7, 81–93. https://doi.org/10.5194/amt-7-81-2014

Moeckli, M.A., Fierz, M., Sigrist, M.W. (1996). Emission factors for ethene and ammonia from a tunnel study with a photoacoustic trace gas detection system. Environ. Sci. Technol. 30, 2864–2867. https://doi.org/10.1021/es960152n

Moravek, A., Murphy, J.G., Hrdina, A., Lin, J.C., Pennell, C., Franchin, A., Middlebrook, A.M., Fibiger, D.L., Womack, C.C., McDuffie, E.E., Martin, R., Moore, K., Baasandorj, M., Brown, S.S. (2019). Wintertime spatial distribution of ammonia and its emission sources in the Great Salt Lake region. Atmos. Chem. Phys. 19, 15691–15709. https://doi.org/10.5194/acp-19-15691-2019

Müller, W., Ölschlegel, H., Schäfer, A., Hakim, N., Binder, K. (2003). Selective Catalytic Reduction - Europe's NOx Reduction Technology. In SAE Technical Paper Series. SAE Technical Paper Series: SAE International400 Commonwealth Drive, Warrendale, PA, United States.

Nowak, J.B., Neuman, J.A., Kozai, K., Huey, L.G., Tanner, D.J., Holloway, J.S., Ryerson, T.B., Frost, G.J., McKeen, S.A., Fehsenfeld, F.C. (2007). A chemical ionization mass spectrometry technique for airborne measurements of ammonia: AIRBORNE CIMS NH 3 MEASUREMENTS. J. Geophys. Res. 112, D10S02. https://doi.org/10.1029/2006JD007589

Nowak, J.B., Neuman, J.A., Bahreini, R., Brock, C.A., Middlebrook, A.M., Wollny, A.G., Holloway, J.S., Peischl, J., Ryerson, T.B., Fehsenfeld, F.C. (2010). Airborne observations of ammonia and ammonium nitrate formation over Houston, Texas. J. Geophys. Res. 115, D22304. https://doi.org/10.1029/2010JD014195

Olivier, J.G.J., Bouwman, A.F., Van der Hoek, K.W., Berdowski, J.J.M. (1998). Global air emission inventories for anthropogenic sources of NO_x, NH_3 and N_2O in 1990. Environ. Pollut. 102, 135–148. https://doi.org/10.1016/S0269-7491(98)80026-2

Olszyna, K.J., Bairai, S.T., Tanner, R.L. (2005). Effect of ambient NH_3 levels on $PM_{2.5}$ composition in the Great Smoky Mountains National Park. Atmos. Environ. 39, 4593–4606. https://doi.org/10.1016/j.atmosenv.2005.04.011

Paulot, F., Jacob, D.J. (2014). Hidden Cost of U.S. agricultural exports: Particulate matter from ammonia emissions. Environ. Sci. Technol. 48, 903–908. https://doi.org/10.1021/es4034793

Peitzmeier, C., Loschke, C., Wiedenhaus, H., Klemm, O. (2017). Real-world vehicle emissions as measured by in situ analysis of exhaust plumes. Environ. Sci. Pollut. Res. 24, 23279–23289. https://doi.org/10.1007/s11356-017-9941-1

Perrino, C., Catrambone, M., Di Menno Di Bucchianico, A., Allegrini, I. (2002). Gaseous ammonia in the urban area of Rome, Italy and its relationship with traffic emissions. Atmos. Environ. 36, 5385–5394. https://doi.org/10.1016/S1352-2310(02)00469-7

Phan, N.T., Kim, K.H., Shon, Z.H., Jeon, E.C., Jung, K., Kim, N.J. (2013). Analysis of ammonia variation in the urban atmosphere. Atmos. Environ. 65, 177–185. https://doi.org/10.1016/j.atmosenv.2012.10.049

Pierson, W.R., Brachaczek, W.W. (1983). Emissions of ammonia and amines from vehicles on the road. Environ. Sci. Technol. 17, 757–760. https://doi.org/10.1021/es00118a013

Pinder, R.W., Adams, P.J., Pandis, S.N. (2007). Ammonia emission controls as a cost-effective strategy for reducing atmospheric particulate matter in the eastern United States. Environ. Sci. Technol. 41, 380–386. https://doi.org/10.1021/es060379a

Puchalski, M.A., Sather, M.E., Walker, J.T., Lehmann, C.M.B., Gay, D.A., Mathew, J., Robarge, W.P. (2011). Passive ammonia monitoring in the United States: Comparing three different sampling devices. J. Environ. Monit. 13, 3156. https://doi.org/10.1039/c1em10553a

R Core Team (2019). R: A language and environment for statistical computing. http://www.r-project.org/index.html

Sakurai, T., Fujita, S. (2002). Analysis of atmospheric ammonia budget for the Kanto region, Japan. Atmos. Environ. 36, 4201–4209. https://doi.org/10.1016/S1352-2310(02)00349-7

Seinfeld, J.H., Pandis, S.N. (2016). Atmospheric chemistry and physics: From air pollution to climate change. 3rd ed., Wiley.

Shen, J., Liu, X., Zhang, Y., Fangmeier, A., Goulding, K., Zhang, F. (2011). Atmospheric ammonia and particulate ammonium from agricultural sources in the North China Plain. Atmos. Environ. 45, 5033–5041. https://doi.org/10.1016/j.atmosenv.2011.02.031

Sudheer, A.K., Rengarajan, R. (2015). Time-resolved inorganic chemical composition of fine aerosol and associated precursor gases over an urban environment in western India: Gas-aerosol equilibrium characteristics. Atmos. Environ. 109, 217–227. https://doi.org/10.1016/j.atmosenv.2015.03.028

Sun, K., Tao, L., Miller, D.J., Pan, D., Golston, L.M., Zondlo, M.A., Griffin, R.J., Wallace, H.W., Leong, Y.J., Yang, M.M., Zhang, Y., Mauzerall, D.L., Zhu, T. (2017). Vehicle emissions as an important urban ammonia source in the United States and China. Environ. Sci. Technol. 51, 2472–2481. https://doi.org/10.1021/acs.est.6b02805

Sutton, M.A, Dragosits, U., Tang, Y.S., Fowler, D. (2000). Ammonia emissions from non-agricultural sources in the UK. Atmos. Environ. 34, 855–869. https://doi.org/10.1016/S1352-2310(99)00362-3

Sutton, M.A., Burkhardt, J.K., Guerin, D., Fowler, D. (1995). Measurement and modelling of ammonia exchange over arable croplands, in: Heij, G.J., Erisman, J.W. (Eds.), Studies in Environmental Science, Elsevier, pp. 71–80. https://doi.org/10.1016/S0166-1116(06)80274-8

Teledyne Advanced Pollution Instrumentation (TAPI) (2012). Model M201E Ammonia Analyzer: Manual Appendum - For use with the M200E Operators Manual, P/N 04410. 05206H DCN5910.

Thoen, E. (2019). padr: Quickly Get Datetime Data Ready for Analysis. R package version 0.5.0. https://CRAN.R-project.org/package=padr

Tsai, J.H., Chang, L.P., Chiang, H.L. (2014). Airborne pollutant characteristics in an urban, industrial and agricultural complex metroplex with high emission loading and ammonia concentration. Sci. Total Environ. 494–495, 74–83. https://doi.org/10.1016/j.scitotenv.2014.06.120

Vogt, E., Held, A., Klemm, O. (2005). Sources and concentrations of gaseous and particulate reduced nitrogen in the city of Münster (Germany). Atmos. Environ. 39, 7393–7402. https://doi.org/10.1016/j.atmosenv.2005.09.012

Wang, C., Tan, J., Harle, G., Gong, H., Xia, W., Zheng, T., Yang, D., Ge, Y., Zhao, Y. (2019). Ammonia formation over Pd/Rh three-way catalysts during lean-to-rich fluctuations: The Effect of the catalyst aging, exhaust temperature, lambda, and duration in rich conditions. Environ. Sci. Technol. 53, 12621–12628. https://doi.org/10.1021/acs.est.9b03893

Wang, M., Kong, W., Marten, R., He, X.-C., Chen, D., Pfeifer, J., Heitto, A., Kontkanen, J., Dada, L., Kürten, A., Yli-Juuti, T., Manninen, H.E., Amanatidis, S., Amorim, A., Baalbaki, R., Baccarini, A., Bell, D.M., Bertozzi, B., Bräkling, S., Brilke, S., … Donahue, N.M. (2020). Rapid growth of new atmospheric particles by nitric acid and ammonia condensation. Nature 581, 184–189. https://doi.org/10.1038/s41586-020-2270-4

Wickham, H. (2009). Ggplot2: Elegant Graphics for Data Analysis. Use R. New York, Springer-Verlag New York. http://dx.doi.org/10.1007/978-0-387-98141-3

Wickham, H. (2019). stringr: Simple, Consistent Wrappers for Common String Operations. R package version 1.4.0. https://CRAN.R-project.org/package=stringr

Wickham, H., Hester, J., Chang, W. (2020). devtools: Tools to Make Developing R Packages Easier. https://CRAN.R-project.org/package=devtools

Wilke, C.O. (2019). cowplot: Streamlined Plot Theme and Plot Annotations for 'ggplot2'. R package version 1.0.0. https://CRAN.R-project.org/package=cowplot

World Health Organization (WHO) (2016). Ambient air pollution: a global assessment of exposure and burden of disease. Geneva, Switzerland.

Xu, J., Chen, Jia, Zhao, N., Wang, G., Yu, G., Li, H., Huo, J., Lin, Y., Fu, Q., Guo, H., Deng, C., Lee, S.-H., Chen, Jianmin, Huang, K. (2020). Importance of gas-particle partitioning of ammonia in haze formation in the rural agricultural environment. Atmos. Chem. Phys. 20, 7259–7269. https://doi.org/10.5194/acp-20-7259-2020

Zhang, H, Wang, J. (2015). Ammonia coverage ratio and input simultaneous estimation in ground vehicle selective catalytic reduction (SCR) systems. J. Franklin Inst. 352, 708–723. https://doi.org/10.1016/j.jfranklin.2014.06.009

Zhang, L., Chen, Y., Zhao, Y., Henze, D.K., Zhu, L., Song, Y., Paulot, F., Liu, X., Pan, Y., Lin, Y., Huang, B. (2018). Agricultural ammonia emissions in China: Reconciling bottom-up and top-down estimates. Atmos. Chem. Phys. 18, 339–355. https://doi.org/10.5194/acp-18-339-2018